Author(s): Delahaye, Julien & Hassel, J. & Lindell, Rene & Sillanpää, Mika & Paalanen, Mikko & Seppä, Heikki & Hakonen, Pertti J.

Title: Low Noise Current Amplifier Based on Mesoscopic Josephson Junction

Year: 2003

Version: Pre-print

Please cite the original version:

Delahaye, Julien & Hassel, J. & Lindell, Rene & Sillanpää, Mika & Paalanen, Mikko & Seppä, Heikki & Hakonen, Pertti J. 2003. Low Noise Current Amplifier Based on Mesoscopic Josephson Junction. Science. Volume 299, Issue 5609. 1-13. DOI: 10.1126/science.299.5609.1045

Low Noise Current Amplifier based on Mesoscopic Josephson Junction

J. Delahaye[1],* J. Hassel[2], R. Lindell[1], M. Sillanpää[1],
M. Paalanen[1], H. Seppä[2], and P. Hakonen[1†]
[1] *Low Temperature Laboratory, Helsinki University of Technology, FIN-02150 Espoo, Finland*
[2] *VTT Information Technology, Microsensing, P.O. Box 1207, 02044 VTT, Finland*

Abstract

We utilize the band structure of a mesoscopic Josephson junction to construct low noise amplifiers. By taking advantage of the quantum dynamics of a Josephson junction, *i.e.* the interplay of interlevel transitions and the Coulomb blockade of Cooper pairs, we create transistor-like devices, Bloch oscillating transistors, with considerable current gain and high input impedance. In these transistors, correlated supercurrent of Cooper pairs is controlled by a small base current made of single electrons. Our devices reach current and power gains on the order of 30 and 5, respectively. The noise temperature is estimated to be around 1 Kelvin, but it is realistic to achieve $T_N < 0.1$ Kelvin. These devices provide quantum-electronic building blocks that will be useful in low-noise, intermediate-impedance-level circuit applications at low temperatures.

* Present address: High Magnetic Field Laboratory LCMI/CNRS BP 166, F-38042 Grenoble, France
† To whom the correspondence should be addressed. E-mail: pertti.hakonen@hut.fi

Charge quantization in nanoelectronic devices is expected to lead to a variety of novel components. The most important invention so far is the single electron transistor (SET) *(1,2)* which presents an unsurpassed charge sensitivity both in the normal and superconducting states *(3)*. Fast SETs are good candidates for read-out devices in solid state quantum computers *(4)*. Owing to its small input capacitance, a SET works extremely well with large source impedances, and various applications of SETs have been proposed accordingly *(5)*.

Superconducting quantum interference devices (SQUID) reach extremely good sensitivity with small impedance sources *(6)*. They are the common choice for measurements trying to approach the standard quantum limit or even attempting to go beyond it. At intermediate impedance values ($\sim$ 1 MΩ) both SETs and SQUIDs run into problems due to impedance mismatch that degrades their performance seriously in this regime.

We present an experimental demonstration of a Bloch oscillating transistor (BOT) that is a good device candidate for intermediate impedance levels. The principle of the device *(7)* takes advantage of the interlevel transition probabilities and relaxation phenomena in a quantum Josephson junction (JJ), whereby it is possible to construct a device in which a small current of single electrons is employed to generate a substantially bigger (super)current of Cooper pairs. In our experiments, a ratio well above 30 has been reached between these two currents.

The quantum behavior of a superconducting junction is described by the Schrödinger equation *(8)*

$$\frac{d^2\psi}{d(\varphi/2)^2} + \left(\frac{E}{E_C} + \frac{E_J}{E_C}\cos\varphi\right)\psi = 0, \tag{1}$$

where φ is the phase difference of the order parameter across the junction, $E_C = \frac{e^2}{2C}$ denotes the Coulomb energy set by the junction capacitance C, and the Josephson coupling energy $E_J = \frac{\hbar}{2e}I_C$ is given by the critical current I_C of the junction. From this Mathieu equation, energy bands (see Fig. 1) should be formed in a similar fashion as for electrons in a periodic potential *(9)*. In the limit of small Josephson coupling, $E_J/E_C << 1$, the width of the lowest band is nearly equal to E_C, while the gap between the first and second band is given by E_J. In the strongly superconducting case, $E_J/E_C \gg 1$, the band width becomes exponentially small with $\exp(-\sqrt{8E_J/E_C})$ and the gap grows as $\sqrt{8E_JE_C}$. The above picture is valid only if the quantum fluctuations of charge are suppressed by a resistance $R_C > R_Q = h/(2e)^2 \sim 6.5$

kΩ in the immediate vicinity of the junction, *i.e.* the lead capacitance is blocked off from the junction.

The basic quantum dynamics of a Josephson junction involves Bloch oscillations and Zener tunneling (illustrated in Fig. 1). Bloch oscillations take place when the state of the junction follows adiabatically its ground state. Under the influence of a weak current bias, charge Q of the Josephson junction runs along the band, which leads to Bloch reflection at the Brillouin zone boundary (indicated by the horizontal line in Fig. 1). This time-correlated tunneling of Cooper-pairs, is characterized by a frequency $f_B = I/2e$ in a current biased JJ.

Zener tunneling occurs when the junction leaves its ground state at the Brillouin zone boundary by tunneling through the forbidden energy gap without a change of charge. As the bias current increases, the probability to cross the band gap by Zener tunneling grows according to the formula ($E_J << E_C$)

$$\Gamma_{\uparrow} = \exp\{-I_Z/I\} \tag{2}$$

where $I_Z = \frac{\pi e E_J^2}{8\hbar E_C}$ *(10)*. Thus, at bias currents $I \sim \frac{\pi E_J}{16 E_C} I_C$, the probability of Zener tunneling becomes substantial.

Relaxation downwards from higher bands can be induced either by intrinsic mechanism at rate $\Gamma_{\downarrow}$ or by external quasiparticle injection Γ_{ext}. If $\Gamma_{\downarrow} << \Gamma_{ext}$, then external, active control of the junction dynamics can be achieved. $\Gamma_{\downarrow}$ is a strong function of the environmental impedance R_C, and it can be made small when $R_C \gg R_Q$ and when T is small *(11)*.

In order to go beyond the regime of Coulomb blockade of Cooper pairs *(12)* and to have a supercurrent I flowing in the JJ, the biasing voltage has to satisfy $V_{bias} > \frac{dE^{(0)}}{dQ} \mid_{max}$, the maximum slope of the lowest band (see point A in Fig. 1). Then the junction will propagate along the lowest level and perform Bloch oscillations in a periodic fashion at f_B. When the current increases, the probability to cross the band gap by Zener tunneling grows. By selecting the ratio of E_J/E_C and the current I properly, one can tune the probability ratio P_{Zener}/P_{Bloch} so that the state of the junction will tunnel into the second band after a few Bloch oscillations, N on average.

Now, if $V_{bias} < \frac{dE^{(1)}}{dQ} \mid_{max}$, the maximum slope of the second band, then the state of the Josephson junction will become stationary on the higher band after Zener tunneling. If there is no intrinsic relaxation ($\Gamma_{\downarrow} \to 0$), the junction will not relax and it will remain stationary, *i.e.*, Coulomb blockaded on the higher band (sitting, *e.g.*, at point B in Fig. 1).

Consequently, there will be no supercurrent in the JJ before relaxation takes place due to externally-induced quasiparticle tunneling which is indicated by the slanted arrow in Fig. 1. After relaxation the junction will resume again the sequence of Bloch oscillations. In this way, a small current of injected quasiparticles results into a $2N$-amplified current of Cooper pairs. The voltage $V_{JJ}(t)$ over the Josephson junction during the principal cycle of the BOT is illustrated on the right hand side of Fig. 1: $V_{JJ}(t)$ varies either sinusoidally at frequency f_B or it is fixed by V_{bias}. The transition from the former to the latter takes place over a time scale set by the R_CC time constant while the opposite happens within the electron tunneling time. The simplest realization of the BOT consists of a Josephson junction (JJ), a normal metal tunnel junction (NIN), and a compact large resistance R_C (Fig. 2).

To estimate the current gain β of the BOT, the relaxation rate due to the base current I_B, $\Gamma_{ext} = \Gamma_B = I_B/e$, can be incorporated into the total downward transition rate (which becomes $\Gamma\downarrow + \Gamma_B$, see Fig. 1). Assuming that $\tau = R_CC$ can be neglected and that I_B flows only when the JJ is Coulomb blockaded, one may write for the BOT gain ($V_C > e/C$)

$$\beta = \frac{dI_C}{dI_B} = \frac{V_C}{eR_C}\frac{1}{\Gamma_\uparrow + \Gamma_\downarrow}. \tag{3}$$

Here I_C denotes the collector current and V_C is the total transport voltage. This equation predicts current gains on the order of 10 at $E_J/E_C = 0.7$ and $T = 0.1$ K. Further details can be found in Ref. *(13)*.

We have also performed more elaborate analysis of the BOT operation based on the application of $P(E)$-theory to the tunneling rates *(14)*. The $P(E)$-theory takes into account probabilities of inelastic tunneling processes in a resistive environment where phase fluctuations are governed by R_C, and thereby it allows us to simulate the operation of the BOT in a more reliable fashion than was possible in the first simulations *(7)* based on the orthodox theory. By taking into account both the inelastic Cooper pair and quasiparticle tunneling, IV-curves similar to the measured ones have been obtained. Contrary to Eq. 3, these simulations show that a small (on the order of 1 nA, strongly dependent on V_C) base current is needed in order to reach $\beta \sim 10$. According to our simulations, the maximum current gain takes place around $E_J/E_C \sim 1$, *i.e.* in a region where the employed approximations ($E_J \ll E_C$) start to break down. Hence, all the reported simulation results in this paper should be considered only as indicative.

Due to technological issues, our practical realization of the BOT is slightly different from

the scheme of Fig. 2. Instead of the NIN junction for injecting quasiparticles we are using a superconductor-normal metal tunnel junction (SIN). This is a somewhat worse choice, but the manufacturing of even such a device is complicated, as it requires a rather elaborate four angle evaporation process *(15)*. The sample structure consists of three elements: an Al-AlO_x-Al Josephson junction (SQUID-like geometry for tunability *(15)*) with tunneling resistance $R_T^{JJ} \cong 5$ kΩ, a superconducting-normal Al-AlO_x-Cu tunnel junction with $R_T^{SIN} \cong 10$ kΩ, and a thin film Cr resistor of $R_C \cong 50$ kΩ (20 μm long), located within a few μm from the two junctions. A scanning electron micrograph of a manufactured BOT device is displayed in the lower part of Fig. 2.

The measured IV-characteristics of a BOT, called H (hysteretic), are illustrated (Fig. 3) at a few values of base current I_B. The voltage V_C denotes the full voltage across the Cr-resistor and the JJ. The base current to the SIN junction is injected via a 100 MΩ bias resistor at room temperature, but this biasing becomes effectively a voltage bias owing to the line capacitance of the coaxial line inside the cryostat. The active region, where I_B has a large influence, is seen to be small, and this region is found to move with increasing I_B. The IV-curves in are slightly hysteretic with respect to the direction of the voltage ramp; only this sample of our three samples *(15)* showed hysteresis. The hysteresis is related with the fact that a variable part of I_B causes only intraband transitions, not relaxation from the upper level (see below).

There is a substantial asymmetry with respect to the polarity of V_C in the IV curves of sample H (see the region where $|V_C|$ is slightly below the hysteresis loop in Fig. 3). At $I_B = +0.8... + 1.2$ nA, the maximum current-induced change is about 10 times larger at $V_C < 0$ than at $V_C > 0$. We consider this asymmetry as a very strong proof that the underlying principle of the BOT operation is working: relaxation due to quasiparticle tunneling can take place only under one polarity *(16)*. If the device would work as a parametric amplifier due to I_B-induced changes in the environmental impedance, then the behavior should be symmetric. The maximum current gain is obtained at $I_B = 1$ nA, which is consistent with our simulations using $P(E)$-theory.

In the measured current gain at $I_B = 1$ nA on a non-hysteretic sample (NH) (Fig. 4), the gain is seen to peak rather strongly with respect to the transport voltage; the peaking of the current gain becomes more and more prominent with increasing value of β. This peaking reflects the strong dependence of Zener tunneling on the external current. One should note,

however, that negative feedback can always be employed to enhance the operating region.

As a function of E_J/E_C, we find a maximum, $\beta \sim 35$, at an optimum ratio of $E_J/E_C = 3.4$. Such a large ratio for E_J/E_C means that higher bands of the junction are involved in the process: the lowest bands are too narrow to present a large-enough Coulomb blockade needed for the BOT operation. This factor has not been taken into account in our simulations yet. Above the optimum ratio, the gain drops quickly. At present, the rapid decrease of gain at large values of E_J/E_C is not understood, and it may be a weakness of our non-optimized first devices.

The other main characteristics of a low-noise amplifier are the available power gain η, the band width BW, the dynamic range A, the optimum input impedance Z_{opt}, and the noise temperature T_N. For the available power gain of sample NH we obtained a value of $\eta = \frac{Z_{out}}{Z_{in}}\beta^2 = 5$ by measuring β, Z_{in}, and Z_{out}. This small value is due to an impedance conversion, *i.e.* due to the fact that the measured input impedance follows $Z_{in} \cong \beta R_C$ while at the output we have $Z_{out} = -30$ kΩ at the optimum operating point. The band width is expected to be limited well below $\min\{1/R_C C, f_B/\beta\} \sim 1$ GHz, set either by the RC time constant or the Bloch oscillation frequency. Note also that the band width restricts the minimum value of I_B since, at least, $I_B > 2eBW$ according to the Nyquist sampling theorem. From the experimental curves in Fig. 4, we obtain for the dynamic range $A = 50$ pA at the largest current gains. At gains on the order of 10, we find $A = 250$ pA.

The noise properties of a BOT are rather involved. This is mostly because the input and output noises are strongly correlated. Consequently, our noise analysis differs slightly from the standard modeling. A BOT has two principal noise sources: the shot noise due to I_B and the broadening of the Bloch oscillation peak caused by the current fluctuations in collector resistance R_C. Owing to charge relaxation via R_C, a BOT is insensitive to $1/f$ background charge fluctuations that hamper the operation of SETs severely.

The width of the Bloch oscillation peak is given by the equation *(8)*

$$\Gamma_B = \left(\frac{\pi}{e}\right)^2 k_B T/R_C. \tag{4}$$

This contribution spreads approximately over the frequency span of 2 GHz at $T = 100$ mK with $R_C = 67$ kΩ. Thus, even though the total power of the Bloch oscillation peak were as high as $(100\ \mu\text{eV})^2$, it amounts only to voltage noise of 2 nV/$\sqrt{\text{Hz}}$. Further away from f_B its contribution becomes smaller and its share can be neglected below 1 GHz. As a matter

of fact, the Bloch peak is so weak and broad that it is barely visible in the Fourier power spectra of our simulated data.

The most detrimental noise contribution is the current fluctuation i_n due to the shot noise of I_B *(17)*. Since it is inherent to the device due to tunneling of electrons at the base, this noise component has to be independent of the source impedance. In our noise model, the source-independence is achieved using a correlated voltage noise generator, $e_n = Z_{in} i_n$, in the input circuit. Optimization with respect to the noise factor *(18)* leads to $Z_{opt} = Z_{in}$ and $T_n = Z_{in} {i_n}^2/k_B = 2eI_B Z_{in}/k_B \sim eV_{in}/k_B$. Typical values for our present samples are $Z_{opt} = 300 - 400$ kΩ and $T_n = 1 - 4$ K calculated for moderate current gains of $\beta = 4 - 6$ at $I_B = 0.2 - 0.4$ nA ($i_n \sim 8 - 11$ fA/$\sqrt{\text{Hz}}$) *(19)*. With $i_n = 10$ fA/$\sqrt{\text{Hz}}$ the relative dynamic range becomes better than 80 dB/$\sqrt{\text{Hz}}$.

T_n may be substantially smaller than the above estimate. According to our simulations, the base current consists of two parts: $I_B = I_{B_1} + I_{B_2}$ where I_{B_1} induces interlevel transitions (relaxation) while I_{B_2} causes only transitions within one band. The ratio I_{B_1}/I_{B_2} depends on the operating point and, typically, we find $I_{B_2} > I_{B_1}$ in our calculations. Since only I_{B_1} produces current gain, we expect $T_n^{calc} \sim 2eI_{B_1} Z_{in}/k_B \ll T_n$. In the hysteretic regime, which vanishes with growing resistance of the base tunnel junction, the ratio I_{B_1}/I_{B_2} has two stable values. Close to the hysteretic region, the devices have a large gain, because, in addition to the change of I_B, there will be an enhancement in output current due to a change in I_{B_1}/I_{B_2}.

In principle, a BOT can be used as a voltage-triggered, single-shot detector at $I_B = 0$. In this mode, a pair of oppositely-biased BOTs can be employed as an "event trigger" detector for charge qubits *(20)*. Unfortunately, only a very small coupling between the qubit and the BOT is tolerated if one wants to equal the decoherence times measured recently by Vion *et. al. (21)*.

The most likely application of the BOT will be a submillimeter-wave detector based on a single tunnel junction, either SIN *(22)* or SIS *(23)*. Using a SQUID read-out with a noise of 50 fA/$\sqrt{\text{Hz}}$ *(24)*, a SIN detector reaches a noise equivalent power of 10^{-18} W/$\sqrt{\text{Hz}}$. Similar noise characteristics are obtained with SIS detectors, for which SET read-outs have been demonstrated to yield $i_n = 15$ fA/$\sqrt{\text{Hz}}$ *(25)*. Our noise estimates for BOTs compare well with these results, even though they are based on first, non-optimal devices. In Ref. 25 it was suggested that single photon counting could be implemented using a quantum-limited

SET for read-out. An optimized BOT might reach the same performance, but in this case, it might be better to use a BOT as a charge multiplier, *i.e.*, in a mode where individual charge pulses in the output are resolved.

BOTs may also find their way into metrology, where the detection and comparison of small quantized currents generated by a Single Electron Tunneling Current Pump is an issue. Ultimately, the goal is to close the quantum triangle by combining Josephson voltage, Quantum Hall resistance and Quantum current standards at the level of relative uncertainty of 10^{-8}. One approach presently is to use an amplifier based on a Cryogenic Current Comparator and a SQUID to multiply the current generated by a SET pump. The equivalent current noise for such a setup has been demonstrated to be 4 fA/$\sqrt{\text{Hz}}$ *(26)*. With a BOT one should reach comparable noise levels, with the further benefit of an on-chip integration of the readout element.

---

1. D.V. Averin, K.K. Likharev, J. Low Temp. Phys. **62**, 345 (1986).
2. T.A. Fulton, G.J. Dolan, Phys. Rev. Lett. **59**, 109 (1987).
3. A. Aassime, D. Gunnarsson, K. Bladh, P. Delsing, R. Schoelkopf, Appl. Phys. Lett. **79**, 4031 (2001).
4. M.H. Devoret, R.J. Schoelkopf, Nature **406**, 1039 (2000).
5. K.K. Likharev, Proc. IEEE **87**, 606 (1999).
6. J. Clarke, in *SQUID Sensors: Fundamentals, Fabrication, and Applications*, H. Weinstock (Ed.), (Kluwer Academic Publisher, Amsterdam, 1996).
7. J. Hassel, H. Seppä, IEEE Trans. Appl. Supercond. **11**, 260 (2001).
8. D. Averin, K.K. Likharev, A.B. Zorin, Sov. Phys. JETP **61**, 407 (1985).
9. See, *e.g.*, G. Schön and A.D. Zaikin, Phys. Rep. **198**, 237 (1990).
10. A.D. Zaikin, I.N. Kosarev, Phys. Lett. A **131**, 125 (1988).
11. A.D. Zaikin, D.S. Golubev, Phys. Lett. A **164**, 337 (1992).
12. D. B. Haviland, L. S. Kuzmin, P. Delsing, T. Claeson, Europhys. Lett. **16**, 103 (1991).
13. J. Delahaye, *et al.*, in *Proceedings of the 23rd International Conference on Low Temperature Physics*, to be published.
14. G.L. Ingold, Yu.V. Nazarov, in *Single Charge Tunneling, Coulomb Blockade Phenomena in*

Nanostructures, ed. by H. Grabert and M. Devoret (Plenum, New York, 1992), p. 21.

15. Materials and methods are available as supporting material on *Science* Online.
16. If quasiparticle tunneling takes place in the opposite direction, the tunneling brings the junction charge Q further away from the background charge Q_0, and the energy will increase according to $\frac{1}{2C}(Q - Q_0)^2$. Consequently, the junction will make a transition to the third energy level.
17. The output current is made of charge pulses of size βe. Therefore, the output current noise is given by $\sqrt{2(\beta e)I_{out}} = \sqrt{2(\beta e)\beta I_B} = \beta\sqrt{2eI_B}$ and this reduces to shot noise of I_B at the input. This contains all the noise, except possible leakage current contributions. The apparent switching voltage noise at the output is given simply by the instantaneous $R_C I_{out}(t)$.
18. A. van der Ziel, *Noise in Solid State Devices and Circuits* (Wiley, New York, 1986), Ch. 3.
19. There is a small noise contribution from the output leakage current ~ 1 nA. Using the measured transconductance $g_m \cong 1/R_c$ (valid when $\beta > 5$), we estimate a contribution of 0.4 K in T_n.
20. Yu. Makhlin, A. Schnirman, G. Schön, Rev. Mod. Phys. **73**, 357 (2001).
21. D. Vion, *et al.*, Science **296**, 886 (2002).
22. M. Nahum, J.M. Martinis, Appl. Phys. Lett. **63**, 3075 (1993).
23. A. Peacock, *et.al.*, Nature **381**, 135 (1996).
24. See, *e.g.*, D. Golubev, L. Kuzmin, J. Appl. Phys. **89**, 6464 (2001).
25. R. J. Schoelkopf, S.H. Moseley, C.M. Stahle, P. Wahlgren, P. Delsing, IEEE Trans. Appl. Supercond. **9**, 2935 (1999).
26. Y. De Wilde, F. Gay, P.M. Piquemal, G. Génevès, IEEE Trans. Instrum. Meas. **50**, 231 (2001).
27. We acknowledge interesting discussions with M. Kiviranta, J. Pekola, J. Penttilä, A. Schakel, and A.D. Zaikin. This work was supported by the Academy of Finland and by the Large Scale Installation Program ULTI-3 of the European Union.

Supporting Online Material

www.sciencemag.org

Materials and Methods

Animation S1

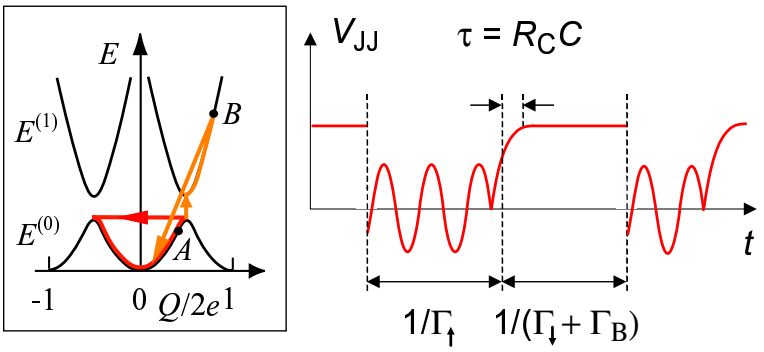

FIG. 1: Basic processes of a BOT in the charge space. Bloch oscillation on the lowest energy band $E^{(0)}$ is denoted by the closed red loop. Occasional Zener tunneling to the second band $E^{(1)}$ is marked by the orange vertical arrow, and the relaxation induced by external quasiparticle injection is illustrated by the slanted orange arrow. On the lowest band, the largest possible voltage across the JJ is at point A, given by $V_{JJ}^{max} = \frac{dE^{(0)}}{dQ}\,|_{max}$; point B denotes the location where $V_{JJ} = V_{bias}$. The right frame displays the voltage of the Josephson junction as a function of time. The upward and downward tunneling rates, $\Gamma_\uparrow$ and $\Gamma_\downarrow$, as well as the quasiparticle tunneling rate Γ_B are discussed in the text. A moving picture of the working cycle of the BOT can be found in Animation S1.

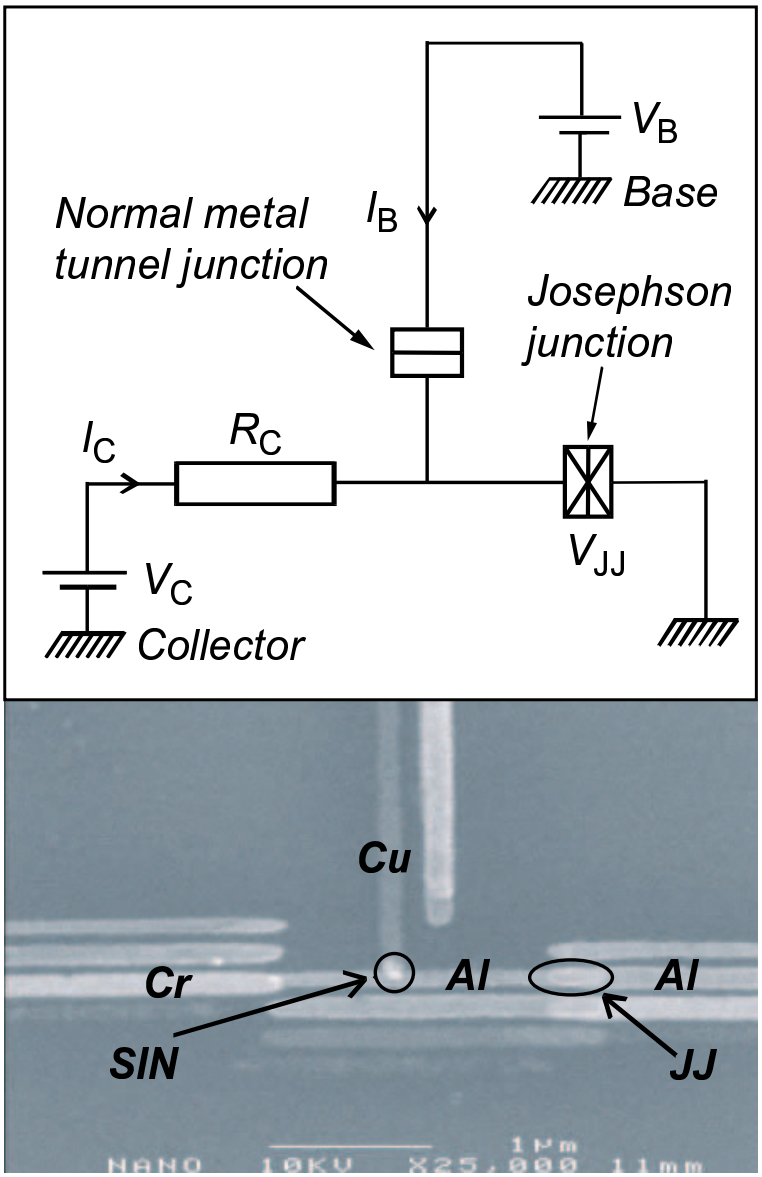

FIG. 2: Implementation of a Bloch oscillating transistor. R_C denotes the collector resistance; bias currents and the corresponding voltage sources are also marked. The lower frame displays a scanning electron micrograph of a manufactured device where the normal metal tunnel junction has been replaced by a SIN (Al-AlO_x-Cu) tunnel junction.

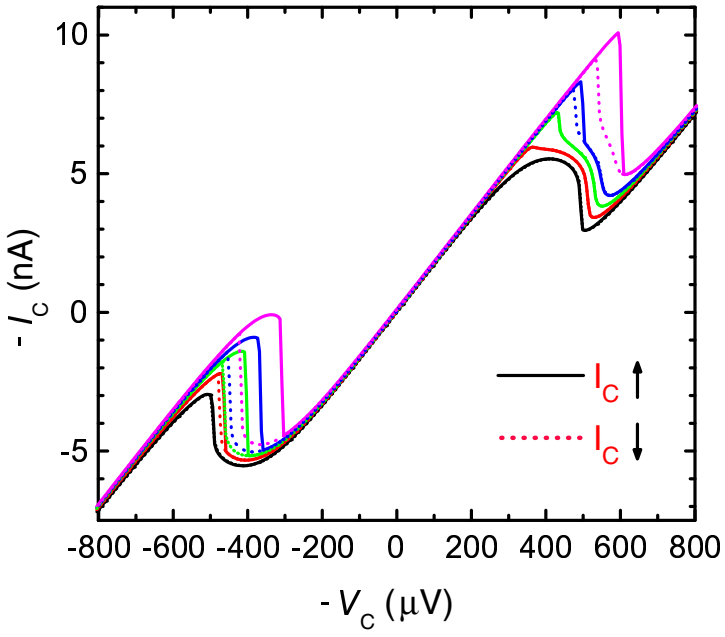

FIG. 3: Current-voltage characteristics for a hysteretic BOT device (H) at base current $I_B = 0$ (black), 0.4 nA (red), 0.8 nA (green), 1.2 nA (blue), and 2 nA (magenta). The parameters of the device read: $E_J = 78$ μeV, $E_C = 50$ μeV, $R_C = 54$ kΩ, $R_T^{JJ} = 7.7$ kΩ, $R_T^{SIN} = 5.8$ kΩ where R_T^{JJ} and R_T^{SIN} refer to the resistances of the Josephson and SIN junctions, respectively. Up and down voltage sweeps are given by the solid and dotted curves, respectively.

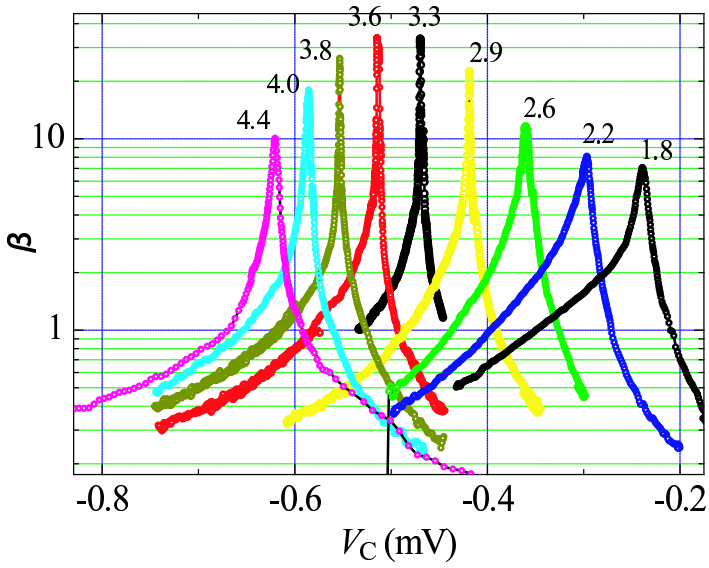

FIG. 4: Current gain measured for a non-hysteretic BOT (NH) when the ratio E_J/E_C is tuned over $1.8-4.4$. The base current was fixed at $I_B = 1$ nA to maximize the current gain. The parameters of the device: $E_J^{max} = 150$ μeV, $E_C = 35$ μeV, $R_C = 67$ kΩ, $R_T^{JJ} = 4.3$ kΩ, $R_T^{SIN} = 10$ kΩ. In this BOT we also had a Cr-resistor of 50 kΩ next to the SIN junction.